OPEN

MRI Dixon Fat-Corrected Look-Locker T1 Mapping for Quantification of Liver Fibrosis and Inflammation—A Comparison With the Non–Fat-Corrected Shortened Modified Look-Locker Inversion Recovery Technique

Jeremias Bendicht Klaus, MD, Ute Goerke, PhD, Markus Klarhöfer, PhD, Mahesh Bharath Keerthivasan, PhD, Bernd Jung, PhD, Annalisa Berzigotti, MD, Lukas Ebner, MD, Justus Roos, MD, Andreas Christe, MD, Verena Carola Obmann, MD, and Adrian Thomas Huber, MD, PhD

Objectives: This study evaluates the impact of liver steatosis on the discriminative ability for liver fibrosis and inflammation using a novel Dixon water-only fat-corrected Look-Locker T1 mapping sequence, compared with a standard shortened Modified Look-Locker Inversion Recovery (shMOLLI) sequence, with the aim of overcoming the limitation of steatosis-related confounding in liver T1 mapping.

Materials and Methods: 3 T magnetic resonance imaging of the liver including the 2 T1 mapping sequences and proton density fat fraction (PDFF) was prospectively performed in 24 healthy volunteers and 38 patients with histologically proven liver fibrosis evaluated within 90 days of liver biopsy. Paired Mann-Whitney test compared sequences between participants with and without significant liver steatosis (PDFF cutoff 10%), and unpaired Kruskal-Wallis test compared healthy volunteers to patients with early (F0–2) and advanced (F3–4) liver fibrosis, as well as low (A0–1) and marked (A2–3) inflammatory activity. Univariate and multivariate logistic regression models assessed the impact of liver steatosis on both sequences.

Results: Dixon_W T1 was higher than shMOLLI T1 in participants without steatosis (median 896 ms vs 890 ms, $P = 0.04$), but lower in participants with liver steatosis (median 891 ms vs 973 ms, $P < 0.001$). Both methods accurately differentiated between volunteers and patients with early and advanced fibrosis (Dixon_W 849 ms, 910 ms, 947 ms, $P = 0.011$; shMOLLI 836 ms, 918 ms, 978 ms, $P < 0.001$), and those with mild and marked inflammation (Dixon_W 849 ms, 896 ms, 941 ms, $P < 0.01$; shMOLLI 836 ms, 885 ms, 978 ms, $P < 0.001$). Univariate logistic regression showed slightly lower performance of the Dixon_W sequence in differentiating fibrosis (0.69 vs 0.73, $P < 0.01$), compensated by adding liver PDFF in the multivariate model (0.77 vs 0.75, $P < 0.01$).

Conclusions: Dixon water-only fat-corrected Look-Locker T1 mapping accurately identifies liver fibrosis and inflammation, with less dependency on liver steatosis than the widely adopted shMOLLI T1 mapping technique, which may improve its predictive value for these conditions.

Key Words: multiparametric magnetic resonance imaging, liver steatosis, liver fibrosis, liver disease, biopsy

(*Invest Radiol* 2024;00: 00–00)

Liver fibrosis develops in response to long-lasting liver injury and can progress to cirrhosis, causing significant morbidity and mortality.[1,2] Early detection of fibrosis allows identifying patients deserving priority in the treatment of liver disease, since etiologic therapy potentially prevents or even reverses fibrosis progression to cirrhosis,[2,3] emphasizing the importance of appropriate diagnostic tests. Although liver biopsy is the gold standard for diagnosis and follow-up of liver fibrosis and inflammation, its invasiveness, risk of complications, and sampling-errors pose limitations.[4–6] Steatosis (increase in fat content in hepatocytes) is another common response to injury in the liver, therefore co-occurring with liver fibrosis in various circumstances, such as alcohol-related, toxic, infectious, and metabolic dysfunction–associated steatotic liver disease (MASLD).[7,8]

Noninvasive diagnostic methods are nowadays widely used for assessing liver fibrosis and steatosis.[9] Imaging techniques, including ultrasound,[10,11] computed tomography,[12,13] and magnetic resonance imaging (MRI),[14,15] offer noninvasive and repetitive assessment of the whole liver volume. Although ultrasound elastography and vibration-controlled transient elastography (FibroScan; Echosens, France) are accurate in staging fibrosis,[16,17] MR elastography (MRE) shows an even higher accuracy, but its specialized and expensive hardware restricts widespread availability.[17–19]

Quantitative T1 relaxation time mapping has emerged as a valuable and fast MRI technique for liver disease detection and staging, which may be combined with other MRI sequences as part of a multiparametric MRI (mpMRI), without the need for specific hardware.[20–24] However, the measured T1 mapping values in the liver are not only affected by fibrosis, but also by inflammation and steatosis.[25] An assessment of liver inflammation and fibrosis in patients with steatotic liver disease is needed for disease characterization, risk stratification, and therapy guidance, but not unequivocally possible with currently available T1 mapping sequences. As steatosis may be accurately quantified with the nowadays widely available and established multiecho Dixon-based proton density fat fraction (PDFF),[26] a T1 mapping sequence should not measure increased T1 time related to steatosis, but rather

Received for publication January 21, 2024; and accepted for publication, after revision, March 2, 2024.

From the Department of Diagnostic, Interventional, and Pediatric Radiology, Inselspital, Bern University Hospital, University of Bern, Bern, Switzerland (J.B.K., B.J., L.E., A.C., V.C.O., A.T.H.); Institute of Forensic Medicine, University of Bern, Bern, Switzerland (J.B.K.); Dr. Kurz Röntgeninstitut AG, Thun, Switzerland (J.B.K.); Siemens Medical Solutions USA, Tucson, AZ (U.G., M.K.); Siemens Medical Solutions USA, New York, NY (M.B.K.); Department of Hepatology, Inselspital, Bern University Hospital, University of Bern, Bern, Switzerland (A.B.); Department of Radiology and Nuclear Medicine, Lucerne Cantonal Hospital, University of Lucerne, Lucerne, Switzerland (L.E., J.R., A.T.H.); and Liver Elastography Center, Translational Imaging Center, Swiss Institute for Translational and Entrepreneurial Medicine, Bern, Switzerland (A.C., V.C.O., A.T.H.).

V.C.O. and A.T.H. shared last authorship.

Conflicts of interest and sources of funding: A.T.H. is currently receiving a project grant (#188591) from SNSF (Swiss National Science Foundation). For the remaining authors, none declared.

Correspondence to: Jeremias Bendicht Klaus, MD, Department of Diagnostic, Interventional, and Pediatric Radiology, Inselspital, Bern University Hospital, University of Bern, Rosenbühlgasse 27, Bern 3010, Switzerland. E-mail: jeremias.klaus@insel.ch.

ISSN: 0020-9996/24/0000–0000
DOI: 10.1097/RLI.0000000000001084

the isolated T1 time of the fat-suppressed water-fraction, which is related to fibrosis and inflammation.

This study aims to evaluate the impact of liver steatosis on the discriminative ability for liver fibrosis and inflammation using a novel Dixon water-only (Dixon_W) fat-corrected Look-Locker T1 mapping sequence, compared with a standard shortened Modified Look-Locker Inversion Recovery (shMOLLI) sequence, to increase the reliability of T1 relaxometry in steatotic liver disease.

MATERIALS AND METHODS

Study Participants

Between May 2020 and January 2023, healthy volunteers and consecutive patients undergoing liver biopsy for the staging of liver disease were prospectively enrolled in our tertiary care center. Participants underwent mpMRI of the liver, with the interval between liver biopsy and mpMRI restricted to a maximum of 90 days. Written informed consent was obtained from all participants. The study received approval from the local ethics review board (cantonal ethics committee Bern, Switzerland) and was conducted in accordance with the Declaration of Helsinki.

Clinical Data Collection

Every participant completed a dedicated questionnaire, supplying data on age, sex, height, and weight, as well as personal medical background. The medical history and a complete workup of liver disease were obtained prior to liver biopsy. The baseline laboratory tests and comorbidities were extracted from the electronic clinical records. For healthy volunteers, baseline laboratory tests were limited to a blood count on the day of the MRI, which was also conducted on liver biopsy patients.

MRI Technique

All liver mpMRIs were performed on a 3 T MR system (Prisma; Siemens Healthineers, Erlangen, Germany) following a fasting period of over 6 hours. The imaging protocol included T1- and T2-weighted sequences, a multiecho qDixon mapping sequence of the whole liver volume for R2* and PDFF measurements, MRE, as well as T1 and T2 relaxometry.

For T1 relaxometry, 2 methods were utilized: a work-in-progress radial Dixon fat-corrected Look-Locker sequence (Dixon_W)[27] and an shMOLLI sequence[28] with a 3-3-5 design. For both sequences, 4 axial slices were acquired at the level of the liver, covering both liver lobes and avoiding partial volume artifacts with the lung at the liver dome. T1 maps were always generated from the same locations. For the shMOLLI sequence, peripheral pulse triggering was used by measuring the pulse on the patient's fingertip, which was not necessary for the Dixon_W sequence.

For the Dixon T1 mapping sequence, the following parameters were used: repetition time (TR) of 5 milliseconds, echo time (TE) of 1.23 milliseconds and 2.46 milliseconds, inversion time (TI) of 30 milliseconds, and flip angle (FA) of 15°. The slice thickness was 8 mm, the gap was 24 mm, the field-of-view (FOV) was 360 × 360 mm, the matrix was 160 × 160 mm, with an in-plane voxel size of 2.3 × 2.3 mm. Acquisition time was 19 seconds, within 1 breath-hold. T1 maps for water (Dixon_W) and fat (Dixon_F) signal were calculated inline after fat-water separation by a 2-point Dixon method.

For the shMOLLI T1 mapping sequence, the following parameters were used: TR of 2.7 milliseconds, TE of 1.12 milliseconds, TI of 180 milliseconds, and FA of 35°. The slice thickness was 8 mm, the gap was 24 mm, the FOV was 307 × 360 mm, the matrix was 144 × 256, with an in-plane voxel size of 1.4 × 2.1 mm. Parallel imaging (GRAPPA) with a PAT factor of 2 was used. Acquisition time was 1:12 minutes, concatenated over 4 breath-holds (1 breath-hold per slice).

Simultaneous mapping of PDFF and R2* was carried out with a single-shot breath-hold multiecho qDixon 3D VIBE sequence with a TR of 9.05 milliseconds; TEs of 1.05 milliseconds, 2.46 milliseconds, 3.69 milliseconds, 4.92 milliseconds, 6.15 milliseconds, and 7.38 milliseconds; and an FA of 4°. The slice thickness was 3 mm, the gap was 0.6 mm, the FOV was 261 × 380 mm, the matrix was 176 × 256 mm, with an in-plane voxel size of 1.5 × 1.5 mm. Parallel imaging (CAIPIRINHA) with a PAT factor of 4 was used. Acquisition time was 17 seconds.

A comparison of the MRI acquisition parameters of the Dixon and shMOLLI T1 mapping sequences is shown in Table 1.

Image Analysis

A board-certified radiologist (J.K.) with 8 years of experience in liver imaging manually outlined an identical region of interest (ROI) on both T1 maps at the same slice and liver location. Care was taken to encompass as much of the liver parenchyma as possible, maintaining a minimal 5 mm distance from the liver border, large blood vessels, and artifacts to avoid partial volume effects (examples in Fig. 1).

Statistical Analysis

Statistical analysis was conducted using GraphPad Prism (version 9.5.1; GraphPad Software Inc, San Diego, CA). Paired Mann-Whitney test and linear regression analysis compared T1 relaxation times between the 2 mapping sequences in participants with and without significant liver steatosis, based on a PDFF cutoff value of 10%. Unpaired Kruskal-Wallis test compared T1 relaxation times of healthy volunteers to patients with early (F0–2) and advanced (F3–4) liver fibrosis, and patients with low (A0–1) and marked (A2–3) inflammation. Univariate logistic regression assessed the 2 sequences separately with T1 relaxation time as variable. Multivariate analysis evaluated the additional impact of PDFF to assess the influence of liver steatosis in both sequences. Results with a P value <0.05 were considered statistically significant.

RESULTS

Study Population

A total of 70 participants underwent prospective enrollment for mpMRI examination. We excluded participants with incomplete mpMRI due to claustrophobia (n = 2) or MRI technical issues on the day of

TABLE 1. Comparison of MRI Acquisition Parameters of the Radial Dixon Fat-Corrected Look-Locker (Dixon LL) and the shMOLLI T1 Mapping Sequences

	Dixon LL	shMOLLI
TR, ms	5	2.7
TE, ms	1.23, 2.46	1.12
TI_{min}, ms	30	180
Flip angle	15°	35°
Slices, n	4	4
Gap, mm	24	24
Slice thickness, mm	8	8
In-plane voxel size, mm	2.3 × 2.3	1.4 × 2.1
FOV, mm	360 × 360	307 × 360
Matrix, mm	160 × 160	144 × 256
PAT	—	2
Acquisition time, min	0:19	1:12
Breath-hold, n	1×	4×

TR, repetition time; TE, echo time; TI, inversion time; FOV, field of view; PAT, parallel acquisition techniques.

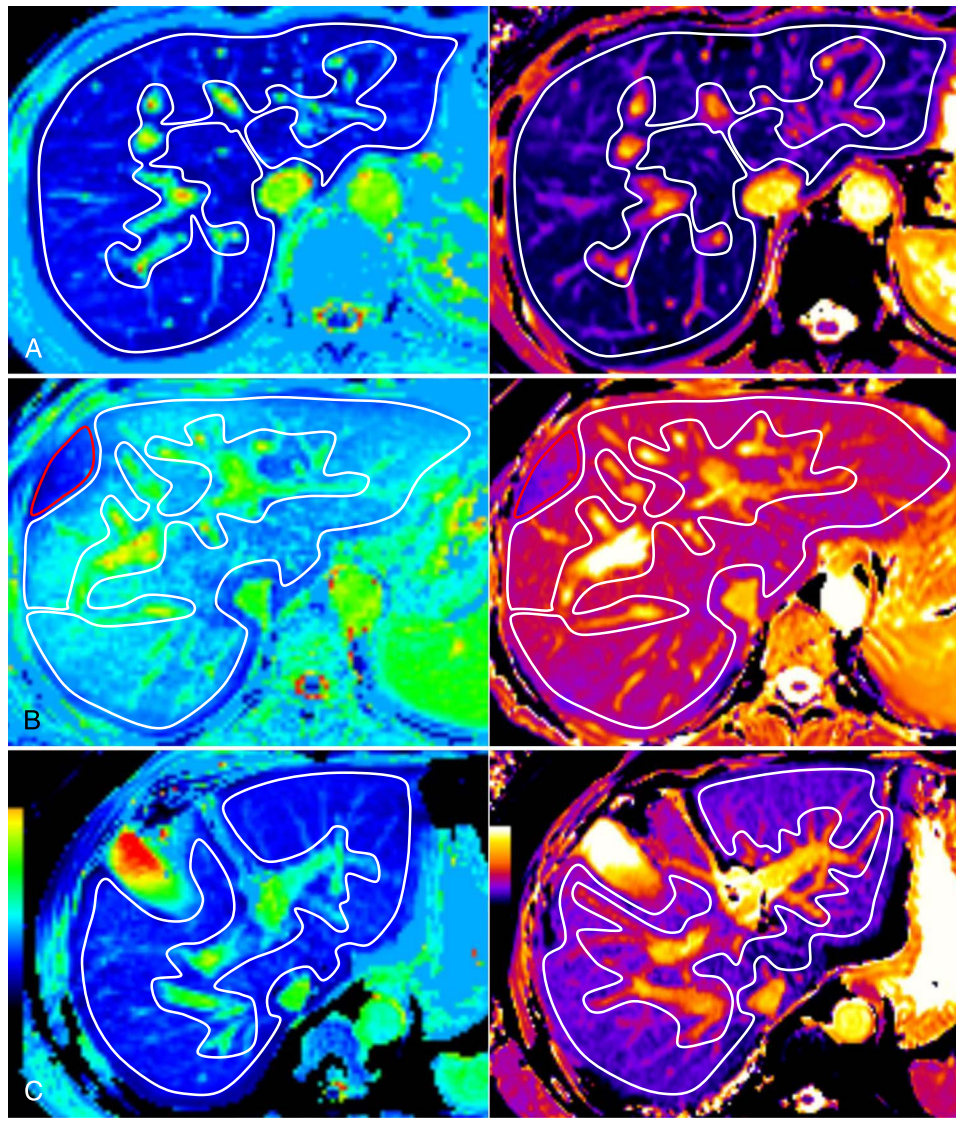

FIGURE 1. T1 relaxation time measurement examples: Dixon_W on the left, shMOLLI on the right. Both maps were each set on the same window width and level values (Dixon_W: L:1350 W:1800/shMOLLI: L:1300 W:1300). Contours of the regions of interest (ROIs) are shown in white. A, A 42-year-old male volunteer without steatosis (PDFF 3%). T1 values: Dixon_W 783 milliseconds, shMOLLI 782 milliseconds. B, A 46-year-old female patient with cirrhosis (F4), severe activity (A3), and mild steatosis (PDFF 9%). T1 values: Dixon_W 1103 milliseconds, shMOLLI 1153 milliseconds. The red contour shows an area with technical artifacts that was excluded from the measurement. C, A 49-year-old male patient with early fibrosis (F1), moderate activity (A2), and moderate steatosis (PDFF 22%). T1 values: Dixon_W 839 milliseconds, shMOLLI 936 milliseconds.

examination (n = 1), hepatic iron overload (>2 mg Fe/g_{dw} based on mpMRI R2* measurement, n = 2), and volunteers with undisclosed health issues at the time of enrollment (n = 2 with arterial hypertension, n = 1 with alcohol consumption exceeding 2 units per day in males and 1 unit per day in females). In total, 62 participants were included: 24 healthy volunteers and 38 patients with histology-proven liver disease (study flowchart in Fig. 2). Among patients, 24 had no or early liver fibrosis (F0 = 6, F1 = 9, F2 = 9) and 14 had advanced liver fibrosis (F3 = 12, F4 = 2), whereas 13 patients showed low inflammation (A0 = 6, A1 = 7) and 25 showed marked inflammation (A2 = 22, A3 = 3).

Participant Characteristics

Participant characteristics are shown in Table 2. Comparisons revealed significant differences in body mass index (BMI) (23 [21–25] kg/m^2 vs 26 [25–33] kg/m^2 vs 30 [28–35] kg/m^2, $P < 0.001$) and PDFF (2 [2–3] % vs 6 [2–17] % vs 10 [8–17] %, $P < 0.001$) between healthy volunteers and patients with early and advanced liver fibrosis. Patients with early liver fibrosis (F0–2) exhibited significantly lower aspartate aminotrasferase (AST) levels (36 [30–49] U/L vs 73 [38–85] U/L, $P = 0.04$), AST-to-platelet ratio index (APRI) scores (0.4 [0.3–0.5] vs 0.9 [0.4–1.3], $P = 0.03$), Fibrosis-4 Index (FIB-4) scores (1.2 [0.9–1.6] vs 2.5 [1.0–3.6], $P = 0.04$), and liver stiffness in the FibroScan (7 [5–10] kPa vs 17 [11–28] kPa, $P < 0.001$) compared with patients with advanced liver fibrosis (F3–4). No significant differences were observed in alcohol consumption, presence of diabetes or arterial hypertension, or levels of alanine aminotrasferase (ALT), gamma-glutamyl transferase (GGT), alkaline phosphatase, bilirubin, albumin, platelets, or creatinine between patient groups.

Impact of Liver Steatosis on T1 Relaxation Times

Dixon_W T1 was higher than shMOLLI T1 in participants without steatosis (median 896 ms [IQR 822–943 ms] vs 890 ms [IQR

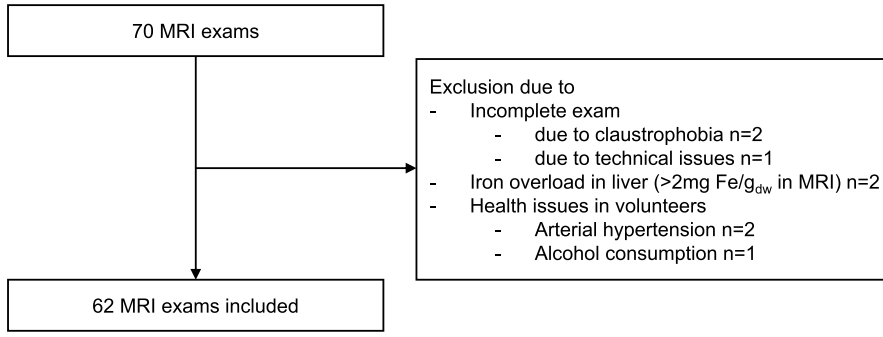

FIGURE 2. Study design flowchart.

798–938 ms], $P = 0.04$), but lower in those with liver steatosis (median 891 ms [IQR 820–1010 ms] vs 973 ms [IQR 901–1139 ms], $P < 0.001$) (Figs. 3A, B). Nevertheless, regression analysis revealed excellent correlation between the 2 sequences, both in participants without steatosis ($r = 0.91$, $P < 0.001$) and with steatosis ($r = 0.99$, $P < 0.001$) (Fig. 3C).

Differentiation of Volunteers and Patients With Early and Advanced Fibrosis

Both Dixon_W and shMOLLI T1 mapping effectively differentiated volunteers from patients with early and advanced fibrosis (Dixon_W: 849 ms, 910 ms, 947 ms, $P = 0.011$; shMOLLI: 836 ms, 918 ms, 978 ms, $P < 0.001$) and those with mild and marked inflammation (Dixon_W: 849 ms, 896 ms, 941 ms, $P < 0.01$; shMOLLI: 836 ms, 885 ms, 978 ms, $P < 0.001$) (Table 3A).

Differentiation of Volunteers and Patients With Mild and Marked Inflammation

Both Dixon_W and shMOLLI T1 mapping methods accurately differentiated between volunteers and patients with mild and marked inflammation (Dixon_W: 849 ms, 896 ms, 941 ms, $P < 0.01$; shMOLLI: 836 ms, 885 ms, 978 ms, $P < 0.001$) (Table 3B).

Combined Analysis of T1 Mapping and PDFF

Univariate logistic regression analysis displayed consistent odds ratios ranging from 1.09–1.10 ($P < 0.01$) for advanced liver fibrosis, corresponding to an 9%–10% probability increase for every 10 milliseconds' elevation in T1 relaxation time (Table 4, univariate model). In the multivariate model, PDFF emerged as an independent predictor for advanced liver fibrosis when combined with T1 relaxation time based on the Dixon_W sequence, but not based on the shMOLLI sequence (Table 4,

TABLE 2. Participant Characteristics

	Volunteers (n = 24)	F0–2 (n = 24)	F3–4 (n = 14)	*P*
Age, y	31 [25–41]	55 [47–62]	52 [43–63]	<0.001
Male, n (%)	11 (46%)	14 (58%)	6 (46%)	0.33
Alcohol consumption, n (%)*	0 (0%)	2 (8%)	1 (7%)	0.93
Diabetes, n (%)	0 (0%)	6 (25%)	4 (31%)	0.93
Arterial hypertension, n (%)	0 (0%)	13 (54%)	3 (23%)	0.67
BMI, kg/m^2	23 [21–25]	26 [25–33]	30 [28–35]	<0.001
PDFF (%)	2 [2–3]	6 [2–17]	10 [8–17]	<0.001
ALT, U/L		57 [36–81]	71 [34–104]	0.62
AST, U/L		36 [30–49]	73 [38–85]	0.04
GGT, U/L		127 [58–262]	149 [55–311]	0.74
Alkaline phosphatase, U/L		101 [70–129]	96 [43–137]	0.5
Bilirubin, µmol/L		8 [6–12]	10 [7–17]	0.34
Albumin, g/L		37 [33–40]	37 [33–40]	0.9
Platelets, 10^9/L		223 [184–286]	194 [156–276]	0.19
Creatinine, µmol/L		72 [59–84]	71 [59–87]	0.99
APRI		0.4 [0.3–0.5]	0.9 [0.4–1.3]	0.03
FIB-4		1.2 [0.9–1.6]	2.5 [1.0–3.6]	0.04
Fibroscan, kPa		7 [5–10]	17 [11–28]	<0.001
A2–3, n (%)		14 (58%)	11 (85%)	0.15

Values are presented as median and IQR [25th–75th percentile] or n.

P values are calculated using a Kruskal-Wallis test for the comparison of 3 groups and an unpaired Mann-Whitney test (for metric data) or Fisher exact test (for categorical data) for the comparison of 2 groups.

*More than 20 g/d for women and more than 30 g/d for men.

AST, aspartate aminotrasferase; ALT, alanine aminotrasferase; GGT, gamma-glutamyl transferase; APRI, AST-to-platelet ratio index; FIB-4, Fibrosis-4 Index; A2–3, METAVIR activity grade; F0–4, METAVIR fibrosis stage.

A

	PDFF <10%	PDFF >10%	*p*-value
n	45	17	
T1 Dixon_W, ms	896 [822-943]	891 [820-1010]	.04
T1 shMOLLI, ms	890 [798-938]	973 [901-1139]	<.001

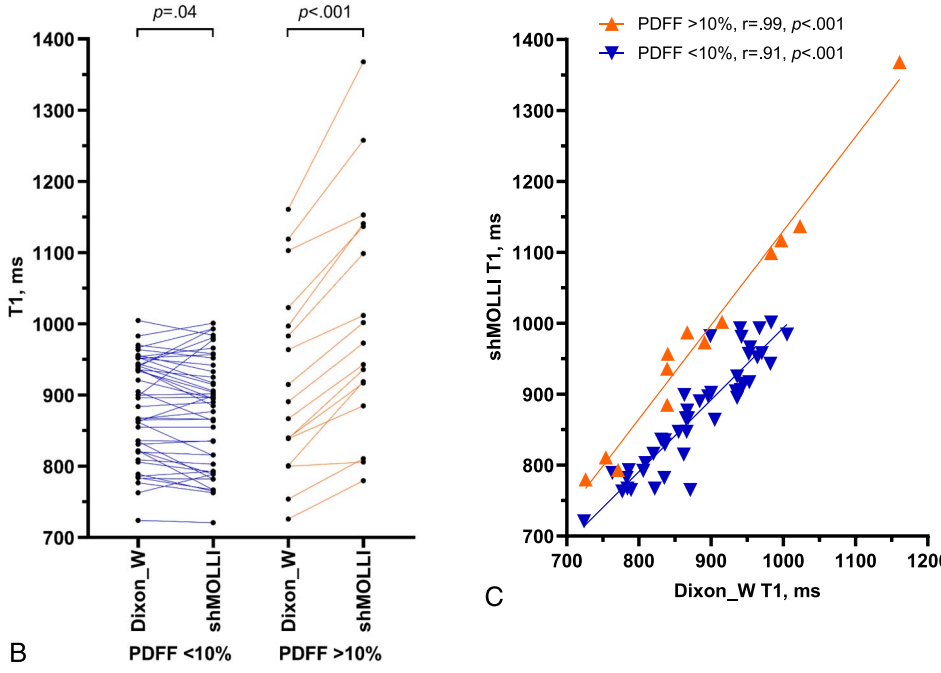

FIGURE 3. Comparison of Dixon_W and shMOLLI T1 mapping techniques as function of hepatic steatosis. A, Descriptive statistics of T1 relaxation times grouped in PDFF <10%/>10%. Values are presented as median and IQR [25th–75th percentile]. B, Paired correlation shows markedly higher T1 relaxation values for shMOLLI in participants with significant steatosis, whereas the values are more similar in the group without steatosis. C, XY correlation. Regression analysis shows excellent correlation between the 2 sequences, both in participants without steatosis and with steatosis.

TABLE 3. Descriptive Statistics for T1 Relaxation Times and PDFF. Values Are Presented as Median and IQR [25th–75th Percentile]

A. Comparison of Healthy Volunteers With Patients With Early (F0–2) and Advanced (F3–4) Liver Fibrosis

	Volunteers	F0–2	F3–4	*P*
n	24	24	14	
T1 Dixon_W, ms	849 [793–926]**	910 [826–953]	947 [851–1024]	0.011
T1 shMOLLI, ms	836 [784–904]***	918 [865–979]*	986 [893–1144]	<0.001
PDFF, %	2 [2–3]	6 [2–17]	10 [8–17]	<0.001
Dixon_W subanalysis: Volunteers vs F3–4**				
shMOLLI subanalysis: Volunteers vs F0–2*, Volunteers vs F3–4***				

B. Comparison of Healthy Volunteers With Patients With Low (A0–1) and Marked (A2–3) Inflammatory Activity

	Volunteers	A0–1	A2–3	*P*
n	24	13	25	
T1 Dixon_W, ms	849 [793–970]*	896 [805–945]	941 [868–983]	<0.01
T1 shMOLLI, ms	836 [784–904]***	885 [796–926]**	978 [912–1007]	<0.001
PDFF, %	2 [2–3]	5 [2–9]	11 [5–17]	<0.001
Dixon_W subanalysis: Volunteers vs A2–3**				
shMOLLI subanalysis: Volunteers vs A2–3***, A0–1 vs A2–3**				

*$P < 0.05$. **$P < 0.01$. ***$P < 0.001$.

F0–4, METAVIR fibrosis stage; A0–3, METAVIR activity grade; Dixon_W, Dixon water-only fat-corrected Look-Locker T1 mapping sequence; shMOLLI, shortened Modified Look-Locker Inversion Recovery T1 mapping sequence.

TABLE 4. Logistic Regression

		Variables								
		T1 (Per 10 ms)			PDFF (Per %)			Area Under the ROC Curve		
ROC Model	Sequence	OR	95% CI	*P*	OR	95% CI	*P*	Area	95% CI	*P*
Univariate	Dixon_W without PDFF as covariable	1.10	1.03–1.20	<0.01				0.69	0.55–0.84	0.02
Univariate	shMOLLI without PDFF as covariable	1.09	1.03–1.17	<0.01				0.73	0.59–0.87	<0.01
Multivariate	Dixon_W with PDFF as covariable	1.11	1.03–1.21	0.01	1.11	1.01–1.22	0.03	0.77	0.64–0.90	<0.01
Multivariate	shMOLLI with PDFF as covariable	1.08	1.02–1.16	0.02	1.05	0.95–1.16	0.3	0.75	0.62–0.89	<0.01

ROC, receiver operating characteristic; PDFF, proton density fat fraction; OR, odds ratio; 95% CI, 95% confidence interval; Dixon_W, Dixon water-only fat-corrected Look-Locker T1 mapping sequence; shMOLLI, shortened Modified Look-Locker Inversion Recovery T1 mapping sequence.

multivariate model). Area under the ROC curve analysis indicated slightly lower performance of the Dixon_W sequence (0.69 vs 0.73, $P = 0.02$ vs $P < 0.01$) based on the univariate logistic regression analysis, which was compensated by adding liver PDFF in the multivariate model (0.77 vs 0.75, $P < 0.01$ for both sequences) (Table 4).

DISCUSSION

The findings of this study provide evidence for the accurate identification of liver fibrosis and liver inflammation by the Dixon_W fat-corrected T1 mapping technique, while demonstrating its reduced susceptibility to the influence of liver steatosis compared with the shMOLLI approach. This highlights the potential of Dixon_W T1 mapping as a valuable noninvasive imaging biomarker, capable of complementing sequences like PDFF in mpMRI to comprehensively characterize liver fibrosis and inflammation. Based on those findings, Dixon_W T1 mapping's advantageous lower collinearity with PDFF may potentially improve its predictive value for assessing liver inflammation and fibrosis, overcoming the limitation of steatosis-related confounding seen with shMOLLI T1 mapping.

Our study reinforces and aligns with limited prior investigations on the impact of fat on liver T1 mapping. Although previous studies identified prolonged T1 relaxation times due to hepatic steatosis with the MOLLI/shMOLLI techniques,[29–31] a few explored water-separated T1 mapping using a variable flip angle gradient echo technique in phantoms and small patient cohorts,[32] assessed gadoxetic acid uptake as a surrogate for liver function,[33] assessed and correlated T1 relaxation times with PDFF in a retrospective study of patients without histologically proven liver disease.[34] In a recent study, the TE dependence of T1 was systematically investigated by comparing a non–fat-corrected (Dixon_IP and Dixon_OP) and a fat-corrected (Dixon_W) Look-Locker sequence in liver steatosis (without histological confirmation).[35] The results confirmed the increase of non–fat-corrected T1 in the presence of liver fat, which was not observed when fat-corrected T1 was measured. We confirmed this observation in our well-characterized study population, which included a large proportion of patients with MASLD. The high proportion of MASLD patients in our study explains the significantly higher BMI, AST, APRI, and FIB-4 score among patients with advanced liver fibrosis compared with those with early liver fibrosis, whereas no significant difference was found in ALT, GGT, alkaline phosphatase, bilirubin, albumin, platelets, or creatinine. Therefore, our findings require confirmation in cohorts involving viral hepatitis, alcohol-related liver disease, and end-stage liver disease. Nonetheless, to our knowledge, this is the first study to systematically compare a fat-corrected Look-Locker sequence (Dixon_W) with the widely adopted non–fat-corrected shMOLLI sequence T1 mapping technique in a prospective study including both healthy volunteers and patients with histologically proven liver disease.

Notably, shMOLLI T1 mapping values alone displayed a nonsignificant tendency to better differentiate patients with and without fibrosis and liver inflammation. This trend may gain statistical significance with a larger patient population. However, this potential shMOLLI advantage was offset upon incorporation of PDFF-based liver steatosis into the multiparametric model. This suggests that the discriminative power of shMOLLI T1 mapping is significantly driven by liver steatosis, closely intertwined with liver fibrosis and inflammation in clinical contexts such as viral hepatitis, alcohol-related liver disease, and MASLD. Consequently, adopting the non–steatosis-biased Dixon_W fat-corrected T1 mapping for a pure multiparametric approach, coupled with PDFF, could offer improved discrimination of liver steatosis, fibrosis, and inflammation. Integrating additional mpMRI sequences such as MRE may further increase the predictive value of mpMRI, especially with artificial intelligence–enhanced liver segmentation[36] and radiomics models.[37] However, whether mpMRI may serve as a noninvasive virtual biopsy warrants external validation and further investigations.

Several limitations merit consideration. The ROI measurements encompassing liver parenchyma included small vessels, potentially introducing partial volume effects, albeit with the exclusion of larger vessels and bile ducts. Furthermore, although the patient cohort was well-characterized through liver MRI, biopsy, and clinical data, it was relatively small and featured a substantial number of patients with grade 3 liver fibrosis in the advanced group. In addition, the cross-sectional analysis of both healthy volunteers and patients with liver disease may introduce selection bias. Consequently, validation within larger, well-characterized patient cohorts with histology-confirmed liver disease is imperative.

CONCLUSIONS

Dixon water-only fat-corrected Look-Locker T1 mapping accurately identifies liver fibrosis and inflammation, with less dependency on liver steatosis than the widely adopted shMOLLI T1 mapping technique.

ACKNOWLEDGMENT

We express our gratitude to Verena Beutler-Minth, Scilla Dozio, Stefan Hüttenmoser, and Marcia Varanda for their support of the study.

REFERENCES

1. Guo J, Friedman SL. Hepatic fibrogenesis. *Semin Liver Dis*. 2007;27:413–426.
2. Hernandez-Gea V, Friedman SL. Pathogenesis of liver fibrosis. *Annu Rev Pathol*. 2011;6:425–456.
3. Campana L, Iredale J. Regression of liver fibrosis. *Semin Liver Dis*. 2017;37:001–010.
4. Khalifa A, Rockey DC. The utility of liver biopsy in 2020. *Curr Opin Gastroenterol*. 2020;36:184–191.
5. Maharaj B, Leary WP, Naran AD, et al. Sampling variability and its influence on the diagnostic yield of percutaneous needle biopsy of the liver. *Lancet*. 1986;327:523–525.

6. Colloredo G, Guido M, Sonzogni A, et al. Impact of liver biopsy size on histological evaluation of chronic viral hepatitis: the smaller the sample, the milder the disease. *J Hepatol*. 2003;39:239–244.
7. Idilman IS, Ozdeniz I, Karcaaltincaba M. Hepatic steatosis: etiology, patterns, and quantification. *Semin Ultrasound CT MR*. 2016;37:501–510.
8. Chan W-K, Chuah K-H, Rajaram RB, et al. Metabolic dysfunction–associated steatotic liver disease (MASLD): a state-of-the-art review. *J Obes Metab Syndr*. 2023;32:197–213.
9. Lurie Y, Webb M, Cytter-Kuint R, et al. Non-invasive diagnosis of liver fibrosis and cirrhosis. *World J Gastroenterol*. 2015;21:11567–11583.
10. Heller MT, Tublin ME. The role of ultrasonography in the evaluation of diffuse liver disease. *Radiol Clin North Am*. 2014;52:1163–1175.
11. Pirmoazen AM, Khurana A, Loening AM, et al. Diagnostic performance of 9 quantitative ultrasound parameters for detection and classification of hepatic steatosis in nonalcoholic fatty liver disease. *Invest Radiol*. 2022;57:23–32.
12. Obmann VC, Mertineit N, Berzigotti A, et al. CT predicts liver fibrosis: prospective evaluation of morphology- and attenuation-based quantitative scores in routine portal venous abdominal scans. *PLoS One*. 2018;13:e0199611.
13. Obmann VC, Marx C, Hrycyk J, et al. Liver segmental volume and attenuation ratio (LSVAR) on portal venous CT scans improves the detection of clinically significant liver fibrosis compared to liver segmental volume ratio (LSVR). *Abdom Radiol (NY)*. 2021;46:1912–1921.
14. Hussain SM, Reinhold C, Mitchell DG. Cirrhosis and lesion characterization at MR imaging. *Radiographics*. 2009;29:1637–1652.
15. Faria SC, Ganesan K, Mwangi I, et al. MR imaging of liver fibrosis: current state of the art. *Radiographics*. 2009;29:1615–1635.
16. Gennisson J-L, Deffieux T, Fink M, et al. Ultrasound elastography: principles and techniques. *Diagn Interv Imaging*. 2013;94:487–495.
17. Zhang YN, Fowler KJ, Boehringer AS, et al. Comparative diagnostic performance of ultrasound shear wave elastography and magnetic resonance elastography for classifying fibrosis stage in adults with biopsy-proven nonalcoholic fatty liver disease. *Eur Radiol*. 2022;32:2457–2469.
18. Huwart L, Sempoux C, Vicaut E, et al. Magnetic resonance elastography for the noninvasive staging of liver fibrosis. *Gastroenterology*. 2008;135:32–40.
19. Darwish OI, Gharib AM, Jeljeli S, et al. Single breath-hold 3-dimensional magnetic resonance elastography depicts liver fibrosis and inflammation in obese patients. *Invest Radiol*. 2023;58:413–419.
20. Margaret Cheng H-L, Stikov N, Ghugre NR, et al. Practical medical applications of quantitative MR relaxometry. *J Magn Reson Imaging*. 2012;36:805–824.
21. Allkemper T, Sagmeister F, Cicinnati V, et al. Evaluation of fibrotic liver disease with whole-liver T1ρ MR imaging: a feasibility study at 1.5 T. *Radiology*. 2014;271:408–415.
22. Banerjee R, Pavlides M, Tunnicliffe EM, et al. Multiparametric magnetic resonance for the non-invasive diagnosis of liver disease. *J Hepatol*. 2014;60:69–77.
23. Hoffman DH, Ayoola A, Nickel D, et al. T1 mapping, T2 mapping and MR elastography of the liver for detection and staging of liver fibrosis. *Abdom Radiol (NY)*. 2020;45:692–700.
24. Obmann VC, Berzigotti A, Catucci D, et al. T1 mapping of the liver and the spleen in patients with liver fibrosis—does normalization to the blood pool increase the predictive value? *Eur Radiol*. 2021;31:4308–4318.
25. Obmann VC, Mertineit N, Marx C, et al. Liver MR relaxometry at 3 T—segmental normal T(1) and T(2)* values in patients without focal or diffuse liver disease and in patients with increased liver fat and elevated liver stiffness. *Sci Rep*. 2019;9:8106.
26. Gu J, Liu S, Du S, et al. Diagnostic value of MRI-PDFF for hepatic steatosis in patients with non-alcoholic fatty liver disease: a meta-analysis. *Eur Radiol*. 2019;29:3564–3573.
27. Keerthivasan MB, Zhong X, Nickel MD, et al. Simultaneous T1 and fat fraction quantification using multi-echo radial Look-Locker imaging. 2020.
28. Piechnik SK, Ferreira VM, Dall'Armellina E, et al. Shortened Modified Look-Locker Inversion recovery (ShMOLLI) for clinical myocardial T1-mapping at 1.5 and 3 T within a 9 heartbeat breathhold. *J Cardiovasc Magn Reson*. 2010;12:69.
29. Mozes FE, Tunnicliffe EM, Pavlides M, et al. Influence of fat on liver T1 measurements using modified Look-Locker inversion recovery (MOLLI) methods at 3 T. *J Magn Reson Imaging*. 2016;44:105–111.
30. Ahn J-H, Yu J-S, Park K-S, et al. Effect of hepatic steatosis on native T1 mapping of 3 T magnetic resonance imaging in the assessment of T1 values for patients with non-alcoholic fatty liver disease. *Magn Reson Imaging*. 2021;80:1–8.
31. Liu C-Y, Noda C, Ambale-Venkatesh B, et al. Evaluation of liver T1 using MOLLI gradient echo readout under the influence of fat. *Magn Reson Imaging*. 2022;85:57–63.
32. Le Y, Dale B, Akisik F, et al. Improved T1, contrast concentration, and pharmacokinetic parameter quantification in the presence of fat with two-point Dixon for dynamic contrast-enhanced magnetic resonance imaging. *Magn Reson Med*. 2016;75:1677–1684.
33. Haimerl M, Probst U, Poelsterl S, et al. Evaluation of two-point Dixon water-fat separation for liver specific contrast-enhanced assessment of liver maximum capacity. *Sci Rep*. 2018;8:13863.
34. Fellner C, Nickel MD, Kannengiesser S, et al. Water–fat separated T1 mapping in the liver and correlation to hepatic fat fraction. *Diagnostics (Basel)*. 2023;13:201.
35. Higashi M, Tanabe M, Yamane M, et al. Impact of fat on the apparent T1 value of the liver: assessment by water-only derived T1 mapping. *Eur Radiol*. 2023;33:6844–6851.
36. Zbinden L, Catucci D, Suter Y, et al. Automated liver segmental volume ratio quantification on non-contrast T1–Vibe Dixon liver MRI using deep learning. *Eur J Radiol*. 2023;167:111047.
37. Defeudis A, Panic J, Nicoletti G, et al. Virtual biopsy in abdominal pathology: where do we stand? *BJR Open*. 2023;5:20220055.